Republic of Iraq
Ministry of Higher Education and Scientific Research
University of Babylon - College of Education for Pure Sciences
Department of Physics

Study of the Effect of Sugar and Food Salt Concentrations in Water on the Absorption of Gamma-Ray Using NaI(Tl) Detector

A research Submitted to the Council of the College of Education for Pure Sciences of University of Babylon in Partial Fulfillment of the Requirements for the Degree of Higher Diploma Education/ Physics of Materials and its Applications.

By

Hawraa Latif Salman Abbas

(B. Sc. in physics 2014)

Supervised by

Ass.Prof. Dr. Inaam Hani Khadhim

University of Babylon - College of Education for Pure Sciences

Department of Physics

2022 A. D. **1444 A. H.**

بسم الله الرحمن الرحيم

مَا كَانَ لِبَشَرٍ أَن يُؤْتِيَهُ اللَّهُ الْكِتَابَ وَالْحُكْمَ
وَالنُّبُوَّةَ ثُمَّ يَقُولَ لِلنَّاسِ كُونُوا عِبَادًا لِّي مِن دُونِ
اللَّهِ وَلَٰكِن كُونُوا رَبَّانِيِّينَ بِمَا كُنتُمْ تُعَلِّمُونَ
الْكِتَابَ وَبِمَا كُنتُمْ تَدْرُسُونَ

صدق الله العلي العظيم

سورة ال عمران (٧٩)

الاهداء

الى النور الذي أنار دربي

والسراج الذي لاينطفي نوره ابدا والذي بذل جهد السنين من اجل ان اعتلي

سلالم النجاح

والدي العزيز رحمه الله

والى من اخص الله الجنه تحت قدميها وغمرتني بالحب والحنان أشعرتني

بالسعادة والأمان هي حياتي وكل عمري

والدتي العزيزه

وإلى رفيق الدرب، وصديق الأيام جميعًا بحلوها ومرّها

زوجي الغالي

أهديكم هذا البحث تعبيرًا عن شكري لدعمكم المستمر.

حوراء

شكر وتقدير

أحمد الله تعالى أولًا وآخرًا على الفضل العظيم الذي منحني إياه، يسرني أن أوجه الشكر الجزيل لكل من نصحني أو أرشدني أو ساهم لو بشيء قليل أو وجهني في إعداد هذا البحث وإيصالي للمراجع والمصادر المطلوبة في أي مرحلة من المراحل التي مررت بها، وأشكر على وجه الخصوص "**أ.م.د أنعام هاني كاظم**"، على مساعدتي ومساندتي وإرشادي بالنصح والتعليم والتصحيح وعلى كل ما بذله معي، كما يسرني أن أشكر "**عمادة كلية التربية للعلوم الصرفة** "، وأسأل الله أن يكون البحث هذا في صحيفة أعالمهم جميعًا، وأن يجزيهم تعالى خير الجزاء والحمد لله رب العالمين.

حوراء

Supervisor Certification

I certify that this research titled " **Study of the Effect of Sugar and Food Salt Concentration in Water on the Absorption of Gamma-Ray Using NaI(Tl) Detector**," was prepared by (**Hawraa Latif Salman Abbas**), under my supervision at Department of Physics, College of Education for Pure Sciences, University of Babylon, as a partial fulfillment of the requirements for the degree of Higher Diploma Education / Physics of Materials and its Application

Signature:

Supervisor: **Dr. Inaam Hani Khadhim**

Title: Assistant Professor

Address: University of Babylon, College of Education for Pure Sciences, Department of Physics.

Date: / /2022

Certification of the Head of the Department

In view of the available recommendation, I forward this research for debate by the Examination Committee.

Signature:

Name: **Dr. Khaled Haneen**

Title: Professor

Address: University of Babylon, College of Education for Pure Sciences, Department of Physics.

Date: / /2022

Scientific Supervisor's Certification

This is to certify that I have read this research, entitled **“Study of the Effect of Sugar and Food Salt Concentration in Water on the Absorption of Gamma-Ray Using NaI(Tl) Detector,"** and I found that this research is qualified for debate.

Signature:

Name: Sameer Hassan Hadi

Title: Professor

Address: University of Babylon, College of Education for Pure Sciences, Department of Physics.

Date: / /2022

Linguistic Supervisor's Certification

This is to certify that I have read this research, entitled **“Study of the Effect of Sugar and Food Salt Concentration in Water on the Absorption of Gamma-Ray Using NaI(Tl) Detector, "** and I found that this research is qualified for debate.

Signature:

Name: Shurooq S. Abid Al-Abas

Title: Professor

Address: University of Babylon, College of Education for Pure Sciences, Department of Physics.

Date: / /2022

Examining Committee Certification

We, the examining committee, certify that we have read the research, "**Study of the Effect of Sugar and Food Salt Concentration in Water on the Absorption of Gamma-Ray Using NaI(Tl) Detector,**" and examined the student **"Hawraa Latif Salman Abbas"** in its contents. We found that it is adequate with ( ) as the research meets the standards for the degree of Higher Diploma Education / Physics of Materials and its Application

Signature:
Name: Dr. Mohanad H. Oleiwi
Title: Professor
Date: / /2022
Chairman

Signature:
Name: Fatima Mohammad Hussain
Title: Assistant Professor
Date: / /2022
Member

Signature:
Name: Dr. Inaam Hani Khadhim
Title: Assistant Professor
Date: / /2022
Supervisor

Approved by the Dean of the college of Education for Pure Science, University of Babylon

Signature:
Name: **Dr. Bahaa Hussien Salih Rabee**
Title: Professor
Date: / /2022

List of Contents

List of Symbols

Symbol	Description
E'	Energy of the scattered photon
E	Incident gamma-ray energy
Θ	Angle of scatter
m_0c^2	Rest mass of the electron
E_e	Energy of electron

List of Figures

List of Tables

Abstract

We have investigated the relationship between the concentrations of salt food and sugar in pure water and the absorption of gamma-ray. The radiation was obtained from radioactive sources and measure by NaI(Tl) detector and Maestro program through studying the parts of the rejoin in energy spectrum. We found that increasing the concentration of table salt with the total area (Gross and Net) of the spectrum decreases, because the water's absorption of radiation passing through it increases with the increase in the concentration of table salt in it, and this leads to a decrease in the total area of the energy spectrum. We note that the relationship is almost linear between the concentration of table salt added and the ability to analyze energy, as increasing the concentration leads to a narrowing in the width of the middle of the top because the width of the middle of the top decreases with the increase in the concentration of salt added. There is an inverse relationship between the concentration of sugar and the total area (Gross and Net) of the spectrum, because the absorbance of water for the radiation passing through it increases with the increase in the concentration of sugar in it, and this leads to a decrease in the total area of the energy spectrum. On the other hand, the relationship between the concentration of the two materials and the ability to analyze energy was found to show linear behavior.

Chapter One

General Introduction

1.1 Introduction

Radiation is emitted from the floor and walls of our homes, the food and drink we consume, and the air we breathe. Alpha particles, beta particles, and gamma rays are the most frequent types of ionizing radiation. Radiation can come from a variety of sources, including natural radio nuclides as well as man-made ones. The gamma ray is an electromagnetic ray that has no charge, so it is no affected by the electric or magnetic field. Gamma rays are emitted from natural and industrial radioactive source in the form of photons .It is characterized by its high penetration [1]. Gamma ray emitted from the isotopes is one of approach which its loss the excitation nuclide from the excess energy to converted these nuclide from high energy level to low energy level that's known radiation decay [2]. NaI(Tl) radiation detectors are robust, low cost spectrometric system (detector and associated electronics) for spectra acquisition and is used at room temperature (no refrigeration), therefore, can be used in various applications in field under unfavorable weather conditions. Detection systems based on these scintillators also have high absorption efficiency for high-energy gamma rays detection due to the relatively high atomic number of Iodine (Z = 53) and, due to the crystal's density, the NaI(Tl) detectors show large absorption efficiency, in other words presents a high photopeak to Compton ratio. When the gamma radiation interacts with the NaI(Tl) detector it yields scintillation that are transformed into electric signal, using a photomultiplier tube that consists of a photocathode that converts photons in the visible light range produced by radiation interaction within the scintillation crystal into electrons that are properly focused and accelerated by the dynodes with which they collide with enough kinetic energy, resulting in secondary electrons[3]. The electron cascade resulting from this multiplication process produces a current pulse that reach the anode of the tube, which is collected with sufficient intensity to be processed in a gamma-ray spectrometry system. These detectors detect radiation by measuring its energy and depend on

the interaction between the nuclear radiation and detector material. The flash detectors are characterized by high absorption[4]. The scintillation detectors for trigger system and neutron time–of flight measurement in the framework of NICA project operated in the strong magnetic field.

1.2 Radioactivity

The term "radioactivity" is used to represent the time rate of disintegration of elements. For any element there exist a certain number of neutrons to proton ratios for it to remain stable, As a result, any deviation from this value will result in an atom that is unstable. By producing energy in the form of radiation, an unstable atom can become stable. Such atoms are said to be radioactive and the process is called radioactivity.

Therefore, natural radioactivity is defined as the spontaneous transformation of unstable nuclei that results in the formation of new elements with the emission of particles and radiations. The most prevalent types of emitted radiation have traditionally been classed as alpha, beta and gamma.

Other types of nuclear radiation include the emission of protons or neutrons, or the spontaneous fission of a large nucleus[5]**.** Alpha and beta particles are ionizing radiation that can only be produced by charged particles. Ionizing radiation is produced indirectly by photons or uncharged particles such as neutrons.

In this situation, ionization happens following the formation of one or more energetic charged particles. By disrupting the DNA in the cell nucleus, all ionizing radiation can have a biological effect[6],[7]. There are two sources of radioactivity (background radiation) as following :

1.3 Natural Source of Radiation

1.3.1 Cosmic Radiation

A radiation stream is created when charged light and star beams contact with the earth's atmosphere and magnetic field. Because of the differences in height and the effects of the world's magnetic field, the amount of cosmic radiation reaches different places of the globe [8]. Cosmic radiation is made out of an incredibly high energy particles (up to $10^{18}eV$), and are for the most part protons (87%), with some bigger particles (alpha radiation 13%). A vast level of it originates from the outside of our solar system and is saved all through space. A portion of the essential enormous radiation evolves from our sun which is created amid sun based flares [9].

1.3.2 Terrestrial Radiation

Terrestrial radiation sources include naturally happening radioactive materials that exist in rocks, soil, water, and vegetation. The uranium series, thorium series, and a single potassium series are the principal isotopes of concern for terrestrial radiation. In different parts of the planet, the amount of radiation from earthly sources varies. Higher portion levels are found in areas with high uranium and thorium concentrations in their soil . With half-lives spanning hundreds of millions of years, they appear to be eternal. Radionuclides with half-lives longer than 30 are not detectable. This section also includes the progeny or rot consequences of long-lived radionuclides [6].The series decay can be classified naturally in three types; including, uranium series (^{235}U), actinium series (^{227}Ac) and thorium series (^{236}Th) see (Figure 1-1). Uranium happens normally as the radioisotopes ^{238}U and ^{235}U which offers rise to decay series that is terminated in the steady isotopes (^{206}Pb and ^{207}Pb), individually. The half-lives of (^{238}U and ^{235}U) are ($4.46x10^{9}$ and $7.13x10^{8}$) years, individually. Thorium happens normally as the radioisotope (Th) which offers rise to decay

series that is terminated in the steady isotope 208Pb (Figure 1-1). The half-lives of (^{232}Th) is ($1.39x10^{10}$) years. Not one or the other (^{238}U, nor ^{232}Th) discharge gamma-rays, and gamma-emissions from their radioactive daughter items are utilized to evaluate their focuses[10] .

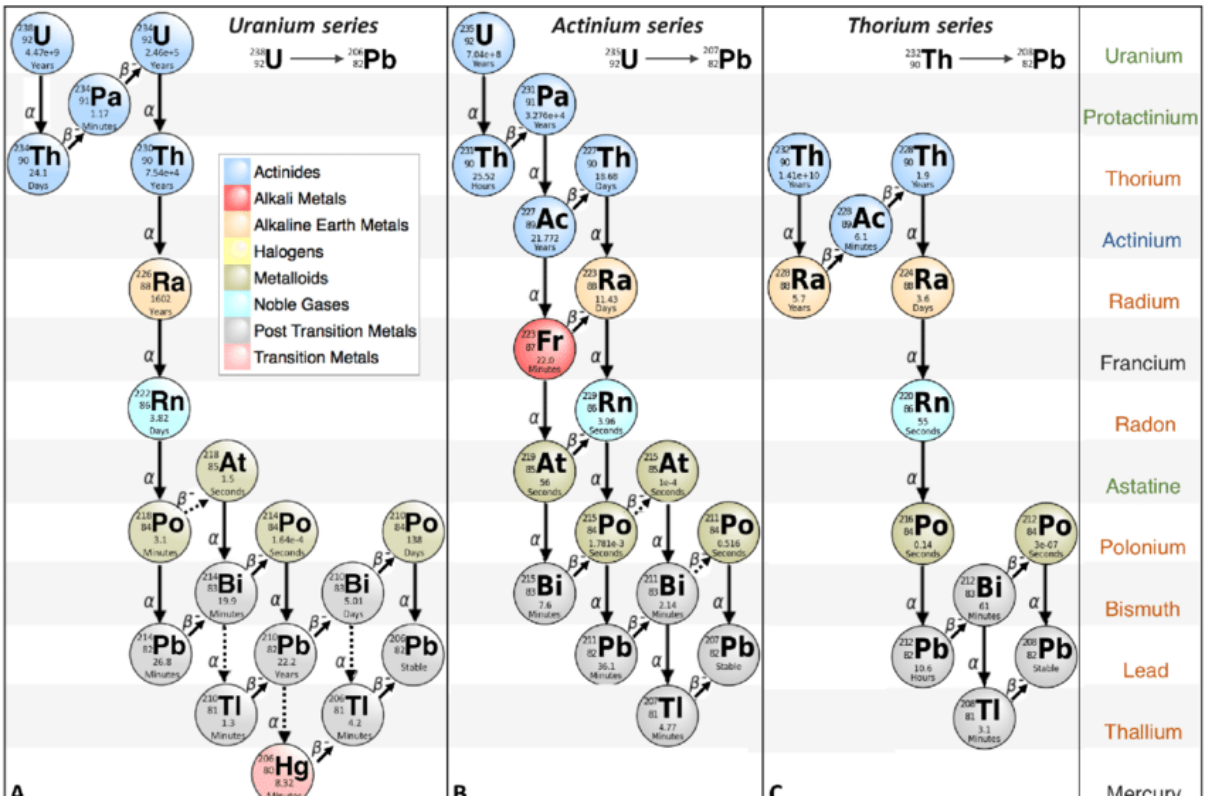

Figure(1-1): ^{238}U, ^{232}Th and ^{235}U decay series[10].

1.3.3 Internal Radiation

Internal radiation is an essential and very important element for the proper function of all organs in the body. It is the substance responsible for the electricity in the body and plays an important role in skeletal . It is made up of radioactive elements that are naturally found in the human body. The essential sources of inward radiation exposures are potassium and carbon. Potassium is a fundamental mineral forever. The potassium ^{40}K isotope (0.01 percent of all potassium) is normally radioactive. It enters the human body through the evolved way of life.

Carbon makes up around 23 percent, by weight, of the human body. Grandiose radiation produces carbon ^{14}C, which is a little level of all carbon. Carbon enters the body through both the evolved way of life and by breathing [11].

1.4 Humans-Invented Radiation Sources

A therapeutic method, such as suggestive X-rays, nuclear drugs, and radiation treatment, is by far the most important source of man-made radiation exposure to the general population. A portion of the significant isotopes would be (^{131}I, ^{99}Tc, ^{60}Co,^{192}Ir, ^{137}Cs, and others). Individuals in the open are exposed to radiation from shopper items, for example, tobacco ($polonium$ ^{210}Po,), building materials, burnable powers (gas, coal), ophthalmic glass, TVs, iridescent watches and dials (tritium), air terminal X-rays frameworks, smoke indicators (americium), street development materials, electron tubes, fluorescent light starters, lamp mantles (thorium), and so on [12].

People who are occupationally exposed are exposed in different ways depending on their jobs and the sources with which they work. Dosimeters, which are pocket-sized equipment that quantify radiation exposure, are used to carefully monitor these people's exposure to radiation. Cobalt-60, cesium-137, americium-241, and other isotopes are among those to be concerned about [13].

1.5 Literature Survey

A. El-Taher in 2013 'Analytical methodology for the determination of concentration of pollutants and radioactive elements in phosphate fertilizer used in Saudi Arabia [14],The measured value of activity concentration of 40K was within the world average range except for NPK fertilizer(mean value 2700Bq kg^{-1}).It is observed that the calculated radium equivalent in fertilizers are lower than the allowed maximum value of 370 Bq kg^{-1} and the calculated $I_\gamma r$ values for NPK and TSP phosphate fertilizers exceed the upper limit for $I_\gamma r$ which is unity

I. Akkurt, et al in 2014[15],The detection Efficiency of NaI(Tl) Detector in 511–1332 keV Energy Range. These study was showed The detection efficiency and energy resolution for the NaI(Tl) scintillation detectors were measured. The variation of detection efficiency with the gamma ray energy and detection distance was also investigated. It was found from this work that the detection efficiency depends on gamma ray energy and also source distance to the detector.

S. Harb, et al in 2015[16], studied Radon exhalation rate and Radionuclides in soil, phosphate, and building materials. In this study the results indicate that phosphate is generally has higher natural radioactivity than other building materials and soil. The exhalation rates are higher for phosphate samples from El Sebaia and lower for marble samples from Qena.

Sudeshna Saha, et al, in 2016, The ammonium molybdate phosphate functionalized silicon dioxide impregnated in calcium alginate for highly efficient removal of ^{137}Cs from aquatic bodies [17], In this study the results are sorption capacity of the material was evaluated as 37.52 mg g^{-1} for cesium at (25–35)℃. Reduction in cesium concentration was carried out without compromising quality of potable water. The beads were generated using NH4OH and capable to be used for a large no. of cycles.

Bibifatima M.Ladhaf, et al, in 2016[18],The effect of Absorber Concentration and Collimator Size on Gamma Ray Attenuation Measurements, In this study the results is the absorption coefficients at 0.112-1.330 MeV of Sorbitol solution explores that increasing concentration makes no considerable change in mass attenuation coefficient values for good geometrical setup (i.e.3.8cm diameter in present case) and for set-ups other than this there is large deviation in experimental and theoretical values(i.e. more than 3%) which cannot be ignored. Also it is observed that collimator size affects the mass attenuation coefficient values

Travis Smith, et al, in 2018[19]. The temporal Fluctuations in Indoor Background Gamma Radiation Using NaI(Tl) , The experimental results showed shields can impact the sensitivity of the detector depending on their detector volume and position inside the shield. This work also investigates when background fluctuations may cause a systematic error when subtracting blank background radiation from sample measurements.

Suresh S., et al, in 2019[20], The studied the measurement of radon concentration in drinking water and natural radioactivity in soil and their radiological hazards, in this study showed The higher radon activity concentrations were observed in bore well and hand pump drinking water samples than the other sources of water. The annual effective dose received by stomach walls through ingestion was significantly low when compared to lung tissues due to breathing of waterborne radon in air. The average activity concentration of ^{226}Ra and ^{232}Th is slightly higher than the world average.

A.S. Alaboodi, et al, in 2020, The studied Radiological hazards due to natural radioactivity and radon concentrations in water samples at Al-Hurrah city, Iraq[21]. Their experimental results showed much lower internal exposures than ICRP reference limits of 1.0 mSv/y and higher than the UNSCEAR reported world average value of 0.12 mSv/y and the WHO reference limits of 0.1 mSv/y, while the use ground water much higher than internal exposures than UNSCEAR, ICRP WHO. Also, it can be concluded according to some radiological parameters such as Raeq, D, Hex, Hin and I_γ were lower than the permissible limit that recommended by UNSCEAR and ICRP, so it may be used in building without and radiation hazard.

Gauri Datar , et al, Causes of the diurnal variation observed in gamma-ray spectrum using NaI (Tl) detector, in 2020[22], the result showed there exists a distinct and significant (> 10%) diurnal pattern in the total number of γ-ray

counts. The counts start decreasing after sunrise and show gradual recovery after sunset. The diurnal pattern is present only in the energies related to the terrestrial background radioactivity (500 keV–2.7 MeV). The study demonstrates that the pattern is associated with the radioactivity of isotopes of radon and their daughter radionuclides.

L. M. Singh, et al, The study of environmental radioactivity and radon measurement associated health effect due to coal and fly ash samples, in 2021[23]. From the study, values of hazard indices are less than one, which concludes that the radiation risk is low in all samples. All parameter values are under the limit prescribed by Radiation Protection Agencies. So, radiation effects around the thermal power plants can is not significant and can neglect. Thus, fly ash appears to be safe, and bricks made from fly ash may be uses as building materials without imposing significant radiological hazards on the public.

Badawi, Mohamed S, et al, in 2022[24], Polymeric composite materials for radiation shielding: a review, in this study the result was showed Using this technique, the geometric, total, and full-energy absorption peak efficiencies, as well as the P/T ratio, can be easily calculated for any source–detector combination.

Abouzeid A.Thabet, et al, in 2022 [25], Analytical-numerical formula for estimating the characteristics of a cylindrical NaI(Tl) gamma-ray detector with a side-through hole, the result showed analytic-numerical formula (ANF) for calculating the geometric solid angle, geometric efficiency, and total efficiency of a cylindrical NaI(Tl) γ-ray detector with a side-through hole. This type of detector is ideal for scanning radioactive fuel rods and pipelines, as well as for performing radioimmunoassay.

1.6 Aims of The Work.

The purpose of this project is to study the relationship between the effect of adding different concentrations of salt food and sugar in pure water on the absorption of gamma rays emitted from radioactive sources, by using NaI(Tl) detector and Maestro program by studying the parts of the rejoin in energy spectrum.

Chapter Two

Theoretical Part

2.1 Introduction

The atomic structure of most elements contains a nucleus that is stable. Under normal conditions, these elements remain unchanged indefinitely. They are not radioactive. Radioactive elements, in contrast, contain a nucleus that is unstable. The unstable nucleus is actually in an excited state that cannot be sustained indefinitely; it must relax, or decay, to a more stable configuration. Decay occurs spontaneously and transforms the nucleus from a high energy configuration to one that is lower in energy. This can only happen if the nucleus releases energy. The energy is emitted by the relaxing nucleus as radiation. All radioactive elements have unstable nuclei; that is what makes them radioactive[26].

2.2 Cesium-137

Cesium is a soft, flexible, silvery-white metal that becomes liquid near room temperature, but easily bonds with chlorides to create a crystalline powder. The most common radioactive form of cesium is Cs-137. Cesium-137 is produced by nuclear fission for use in medical devices and gauges. It is also one of the byproducts of nuclear fission processes in nuclear reactors and nuclear weapons testing[27].

2.2.1 Cesium in the Environment

Because Cs-137 bonds with chlorides to make a crystalline powder, it reacts in the environment like table salt (sodium chloride):[28]

- Cesium moves easily through the air.
- Cesium dissolves easily in water.
- Cesium binds strongly to soil and concrete, but does not travel very far below the surface.

- Plants and vegetation growing in or nearby contaminated soil may take up small amounts of Cs-137 from the soil.

Small quantities of Cs-137 can be found in the environment from nuclear weapons and from nuclear reactor accidents[28].

2.2.2 Cesium Sources

Cesium-137 is used in small amounts for calibration of radiation detection equipment, such as Geiger-Mueller counters. In larger amounts, Cs-137 is used in[29]:

- Medical radiation therapy devices for treating cancer.
- Industrial gauges that detect the flow of liquid through pipes.
- Other industrial devices that measure the thickness of materials such as paper or sheets of metal.

2.2.3 Cesium and Health

External exposure to large amounts of Cs-137 can cause burns, acute radiation sickness and even death. Exposure to such a large amount could come from the mishandling of a strong industrial source of Cs-137, a nuclear detonation or a major nuclear accident. Large amounts of Cs-137 are not found in the environment under normal circumstances. Exposure to Cs-137 can increase the risk for cancer because of the presence of high-energy gamma radiation. Internal exposure to Cs-137 through ingestion or inhalation allows the radioactive material to be distributed in the soft tissues, especially muscle tissue, which increases cancer risk[30].

2.3 Cobalt-60

Cobalt is a hard, gray-blue metal that is solid under normal conditions. Cobalt is similar to iron and nickel in its properties and can be magnetized like iron. The most common radioactive isotope of cobalt is cobalt-60 (Co-60).

Cobalt-60 is a byproduct of nuclear reactor operations. It is formed when metal structures, such as steel rods, are exposed to neutron radiation[31].

2.3.1 Cobalt in the Environment

There are very small amounts of Co-60 in the environment from nuclear facilities. Nuclear Regulatory Commission regulations allow discharge of small amounts of Co-60 from licensed facilities[32].

2.3.2 Cobalt Sources

Cobalt-60 is used as a radiation source in many common industrial applications, such as in leveling devices and thickness gauges. It is also used for radiation therapy in hospitals. Accidental exposures may occur as the result of loss or improper disposal of medical and industrial radiation sources. Though relatively rare, exposure has also occurred by accidental mishandling of a source at a metal recycling facility or steel mill.Most exposure to Co-60 takes place intentionally during medical tests and treatments. Such exposures are carefully controlled to avoid adverse health impacts and to maximize the benefits of medical care[33].

2.3.3 Cobalt and Health

Because it decays by gamma radiation, external exposure to Co-60 can increase cancer risk. Most Co-60 that is ingested is excreted in feces; however, a small amount is absorbed by the liver, kidneys and bones. Cobalt-60 absorbed by the liver, kidneys, or bone tissue can cause cancer from internal exposure to gamma radiation. Mishandling of a large industrial source of Co-60 could result in an external exposure large enough to cause skin burns, acute radiation sickness or death[34].

2.4 NaI(Tl) detectors

The thallium-activated sodium iodide detector, or NaI(Tl) detector, responds to the gamma ray by producing a small flash of light, or a scintillation. The scintillation occurs when scintillator electrons, excited by the energy of the photon, return to their ground state. The detector crystal is mounted on a photomultiplier tube which converts the scintillation into an electrical pulse. The first pulse from the photocathode is very small and is amplified in 10 stages by a series of dynodes to get a large pulse. This is taken from the anode of the photomultiplier, and is a negative pulse.

The NaI(Tl) crystal is protected from the moisture in the air by encasing it in aluminum, which also serves as a convenient mounting for the entire crystal/photomultiplier unit. A schematic is shown in Figure (2-1)[35].

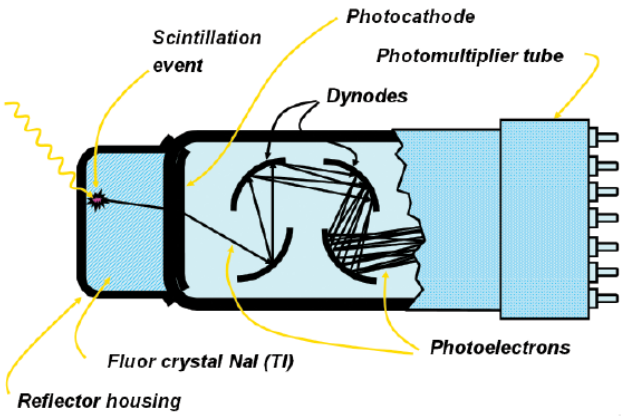

Figure (2-1): illustration of a scintillation event in a photomultiplier tube [35].

2.4.1 Gamma-ray interactions with matter

There are three dominant gamma-ray interactions with matter:

- Photoelectric effect
- Compton effect
- Pair production

The photoelectric effect is a common interaction between a low-energy gamma ray and a material. In this process the photon interacts with an electron in

the material losing all of its energy. The electron is ejected with an energy equal to the initial photon energy minus the binding energy of the electron. This is a useful process for spectroscopy since an output pulse in a detector is produced that is proportional to the gamma-ray energy, as all of the energy of the gamma ray is transferred to the detector. This produces a characteristic full-energy peak in the spectrum that can be used for the purpose of identifying the radioactive material[36].

The photon can scatter by a free electron and transfer an amount of energy that depends on the scattering angle. This process is called Compton scattering. The energy of the scattered photon E′ is:[37]

$$E' = \frac{E}{1 + \frac{E}{m_0 c^2}(1 - cos\theta)} \text{ ----------(1)}$$

where E is the incident gamma-ray energy and θ is the angle of scatter. The term m_0c^2 is the rest mass of the electron, equal to 511 keV. The energy given to the electron is:[38]

$$E_e = E - E' \text{ ----------(2)}$$

The maximum energy given to an electron in Compton scattering occurs for a scattering angle of 180°, and the energy distribution is continuous up to that point (since all scattering angles up to 180° are possible). This energy, known as the Compton edge, can be calculated from the incident gamma ray energy.

For θ = 180°:

$$E' = \frac{E}{1 + \frac{2E}{m_0 c^2}} \text{ ----------(3)}$$

and:

$$E_e = E - E' = E - \left[\frac{E}{1 + \frac{2E}{m_0 c^2}}\right] \text{----------(4)}$$

The spectrum for ^{137}Cs shows that if the gamma ray scatters and escapes the crystal then the energy deposited will be less than the full-energy peak[38].

The actual energy deposited depends upon the angle of scatter as described in the equations above. The spectrum shows that many pulses have energies in a range below the Compton edge – called the Compton Continuum[39]. If the gamma ray does not escape the crystal and scatters again giving up its remaining energy through the photoelectric effect, then its full energy will be deposited in the full-energy peak (at 662 keV for ^{137}Cs). This is more likely for larger crystals. Pair production can occur when the gamma-ray energy is greater than 1.022 MeV and is a significant process at energies above 2.5 MeV. The process produces a positron and electron pair that slow down through scattering interactions in the material. When the positron comes to rest, it annihilates with an electron producing a pair of 511 keV gamma rays that are produced back-to-back. These can be absorbed through the photoelectric effect to produce full-energy peaks at 511 keV. A component due to Compton scattering can also be observed. When a photon interacts with the crystal through pair production, one or both of the annihilation photons can escape undetected from the crystal[40]. If one of the photons escapes undetected, then this will result in a peak in the spectrum at an energy of 511 keV less than the full-energy peak. This is called the single escape peak. Similarly, if both photons escape undetected, a peak will appear 1022 keV below the full-energy peak, called the double escape peak[41].

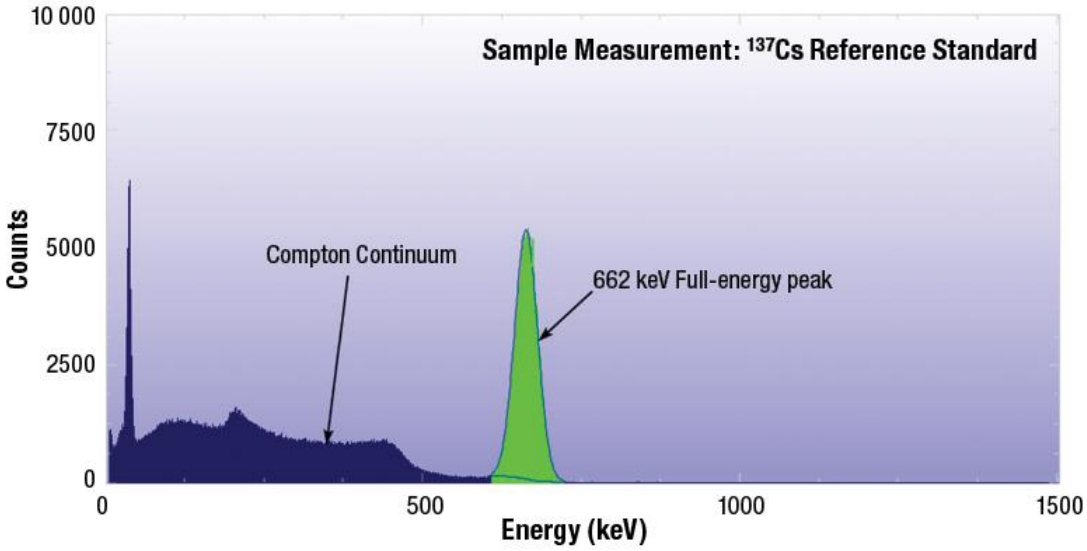

Figure (2-2): Example spectrum of a ^{137}Cs source[40].

Chapter Three

Results and Discussion

3.1 Introduction

This chapter deals with the calculations and results that were obtained in this study using sodium iodide activated thallium detector. NaI(Tl) and using two radioactive sources (^{137}Cs and ^{60}Co). Concentrations of both substances (salt and sugar) were taken starting from (5-50) gm for each a substance for both radioactive sources, and the measurement time was 500 sec for one concentration.

3.2 Study of the energy spectrum regions of gamma rays in salt's mass using A-^{137}Cs source.

The areas of the gamma ray spectrum were studied using the radioactive ^{137}Cs source at a distance of (2 cm) between the detector and the radioactive source, and (300 ml) of pure water was added to the salt mass as in Table.(3-1)

Table(3-1) Studying the regions of the energy spectrum using a radioactive Cesium source and salt table

Mass (gm/cm^3)	Gross area (C/s)	Net area (C/s)	F.W.H.M	Centroid	E.R%
0	651703	620032	79.13	118	0.67
5	608176	551788	78.81	117	0.673
10	602677	551337	77.58	117	0.66
15	552298	475830	75.46	115	0.656
20	523820	424685	74.49	114	0.653
25	495072	418600	74.28	113	0.65
30	494248	411450	73.95	112	0.66
35	486737	397484	72.65	111	0.65
40	486161	395039	71.36	110	0.64
45	485338	368678	70.91	108	0.65
50	482939	328907	65.89	107	0.61

Table (3-1) shows the effect of the mass of salt added to pure water on the absorbance of gamma rays using a cesium source, where the total area of the

optical peak with energy ($662\ keV$) (Gross area) and the net area (Net area) was studied, in addition to calculating Energy analysis capability (E.R) by calculating mid-peak width (F.W.H.M) and optical peak location (Centroid). We notice from the table how the mass of table salt added to ($300\ ml$) of pure water changes over the spectrum areas, as shown in Figures (3-1), (3-2). Note that the zero reading means calculating pure water without adding a concentration of table salt, then gradually adding ($5\ gm$) to the water and calculating the resulting spectrum after ($500\ sec$).

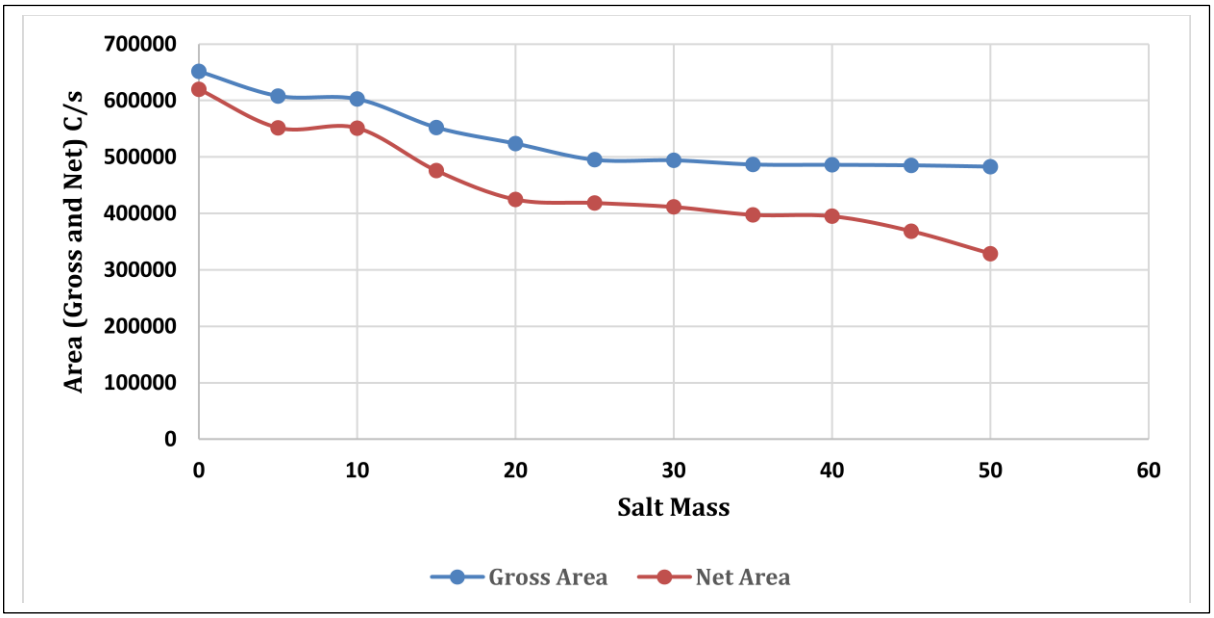

Figure (3-1): The relationship between the change in the mass of table salt and the total area of the energy spectrum using a radioactive Cesium source.

Figure (3-1) shows the relationship between the mass of table salt added to ($300\ ml$) of pure water on the total area of the radioactive Cesium source spectrum for each of the total area of the spectrum (gross area) of the optical peak (the first series in blue) in addition to the net total area (Net Area) of the optical peak (in red).

We note that the relationship was inverse, that is, with an increase in the concentration of table salt, the total area (Gross and Net) of the spectrum decreases, because the absorbance of water for the radiation passing through it

increases with the increase in the concentration of table salt in it, and this leads to a decrease in the total area of the energy spectrum.

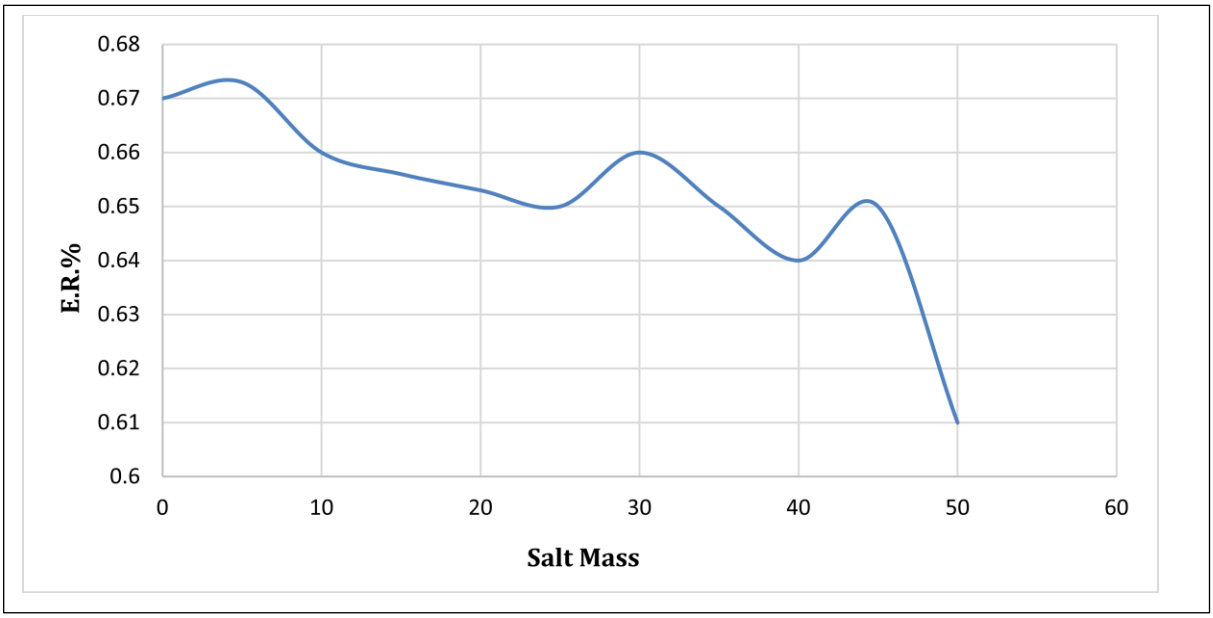

Figure (3-2): The relationship between the change in the mass of table salt and the ability to analyze energy using a radioactive Cesium source.

Figure (3-2) shows the relationship between the mass of table salt added to ($300\ ml$) of pure water on the ability to analyze the energy of the radioactive cesium source spectrum. The peak was between constant and decreasing with the increase in the concentration of added salt, which led to the lack of clarity on the relationship of the ability to analyze energy with the concentration of table salt well added.

3.3 Study of the energy spectrum regions of gamma rays in salt's mass using B- ^{60}CO source.

The gamma ray spectrum regions were studied using the ^{60}Co source at a distance of (2 cm) between the detector and the radioactive source, and (300 ml) of pure water was added to the salt mass as in Table (3-2).

Table(3-2) Studying the regions of the energy spectrum using a radioactive Cobalt source and salt table

Mass (gm/cm^3)	Peak1					Peak2				
	Gross area (C/s)	Net area (C/s)	F.W.H.M	Ce.	E.R.%	Gross area	Net area	F.W.H.M	Ce.	E.R.%
0	25146	16486	91.51	183	0.50	19936	14199	95.98	209	0.45
5	24565	16238	91.13	182	0.50	19208	14031	93.14	209	0.445
10	24418	15694	91.09	182	0.50	19163	13886	92.32	208	0.443
15	24271	15680	89.01	179	0.49	18930	13166	90.14	207	0.43
20	23895	14781	86.51	178	0.486	18896	12439	88.01	207	0.42
25	23092	13975	85.39	178	0.47	18889	12291	85.97	206	0.41
30	23088	13551	84.50	175	0.48	18582	10857	80.68	206	0.39
35	22821	12475	79.15	174	0.45	18222	9892	79.32	204	0.38
40	21983	11964	79.09	173	0.45	17729	8749	75.53	203	0.37
45	21921	11217	74.06	171	0.43	17679	8280	71.58	197	0.363
50	20404	7743	62.98	170	0.37	17016	7530	70.92	197	0.36

Table (3-2) shows the effect of the mass of table salt added to pure water on the absorption of gamma rays using the cobalt radioactive source, where the (Gross area) of the two optical peaks (1173 keV and 1332keV) as well as (Net area), in addition to (E.R.) were studied. . We notice from the table how the mass of table salt added to (300 ml) of pure water changes over the spectrum regions, as shown in Figures (3-3) and (3-4).

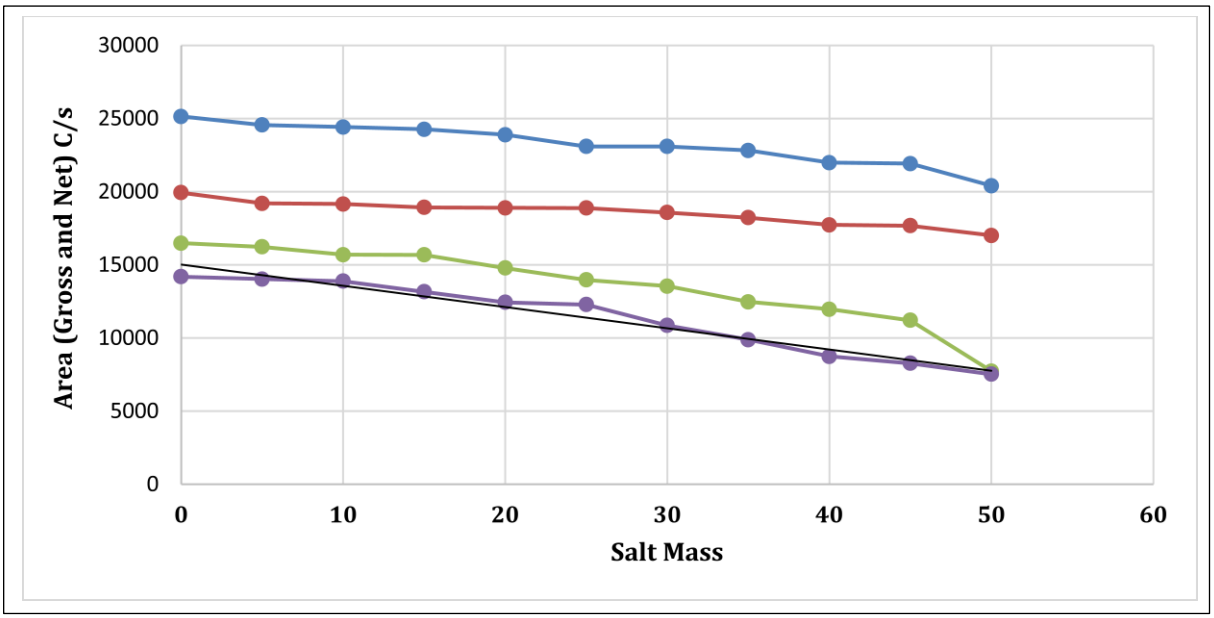

Figure (3-3): The relationship between the change in the mass of table salt and the total area of the energy spectrum using a radioactive Cobalt source.

Figure (3-3) shows the relationship between the mass of table salt added to ($300\ ml$) of pure water on the net total area of the radioactive cobalt source spectrum for each of the Gross Area of the first optical peak (the first series in blue) as well as for the optical peak The second in red (the second series) in addition to the net optical area (Net Area) of the first two optical peaks (in green) and the second optical peak (in violet), where we note that the relationship was inverse between the concentration of table salt with the total area of the spectrum (Gross and Net), i.e. With increasing concentration, the total area of the spectrum decreases for the same reason mentioned in Figure (3-1).

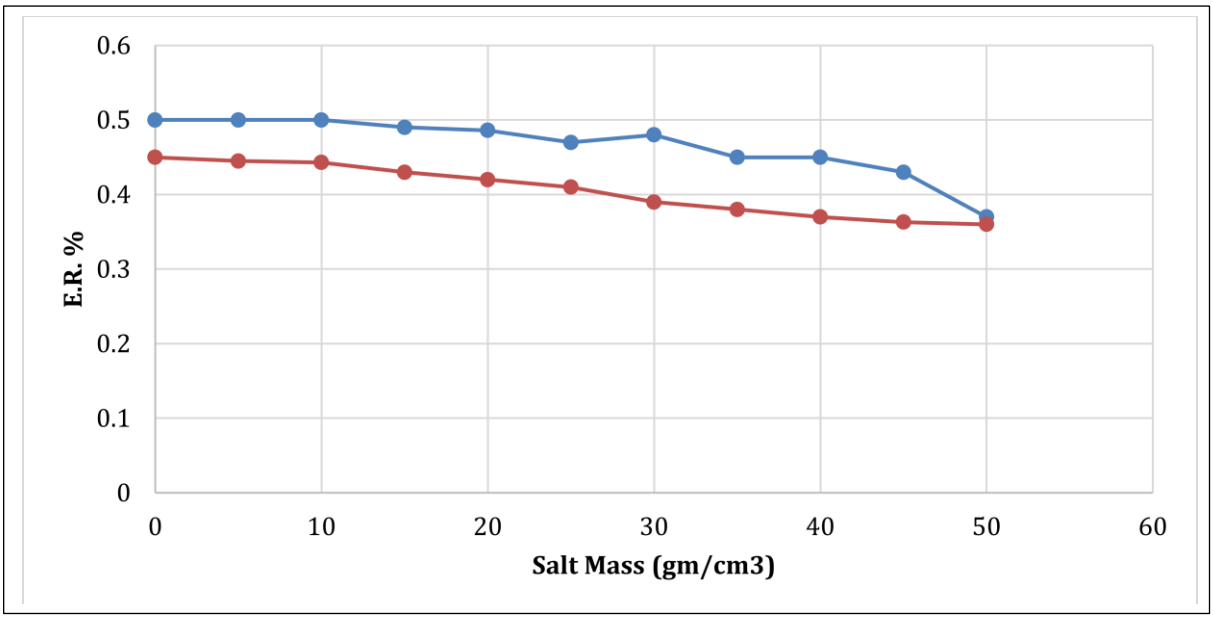

Figure (3-4): The relationship between the change in the mass of table salt and the ability to analyze energy using a radioactive Cobalt source.

Figure (3-4) shows the relationship between the mass of table salt added to ($300\ ml$) of pure water on the ability to analyze the energy of the cobalt source spectrum for the first (blue color) and the second (red color) peaks. Where we note that the relationship is almost linear between the concentration of the added salt and the ability to analyze energy, as increasing the concentration leads to a narrowing in the width of the middle of the peak as well as the widening of the middle of the peak decreases with the increase in the concentration of the added salt, but the location of the peak was between constant and decreasing with the increase in the concentration of the added salt.

3.4 Study of the energy spectrum regions of gamma rays in sugar's mass using A-^{137}Cs source.

The gamma ray spectrum regions were studied using the radioactive ^{137}Cs source at a distance of (2 *cm*) between the detector and the radioactive source, and (300 ml) of pure water was added to the sugar mass as in Table (3-3).

Table(3-3) Studying the regions of the energy spectrum using a radioactive Cesium source and sugar

Mass (gm/cm^3)	Gross area (C/s)	Net area (C/s)	F.W.H.M	Centroid	E.R.%
0	669834	636017	79.98	114	0.701
5	617667	5594702	79.90	114	0.70
10	602238	543331	79.65	114	0.69
15	562336	531424	79.60	113	0.704
20	547764	480429	78.72	113	0.69
25	521306	470485	77.16	112	0.688
30	505527	424339	75.64	111	0.68
35	479564	395096	75.31	110	0.684
40	467279	387587	74.61	108	0.69
45	448535	376396	73.28	107	0.684
50	430030	318471	73.17	106	0.69

Table (3-3) shows the effect of the mass of sugar added to (300 ml) of pure water on the absorbance of gamma rays using a radioactive cesium source, where the (Gross area) of the optical peak with energy (662 keV) was studied as well as the calculation of (Net area), in addition to to (E.R.). We note from the table how the mass of added sugar changes over the regions of the spectrum, as shown in Figures (3-5), (3-6).

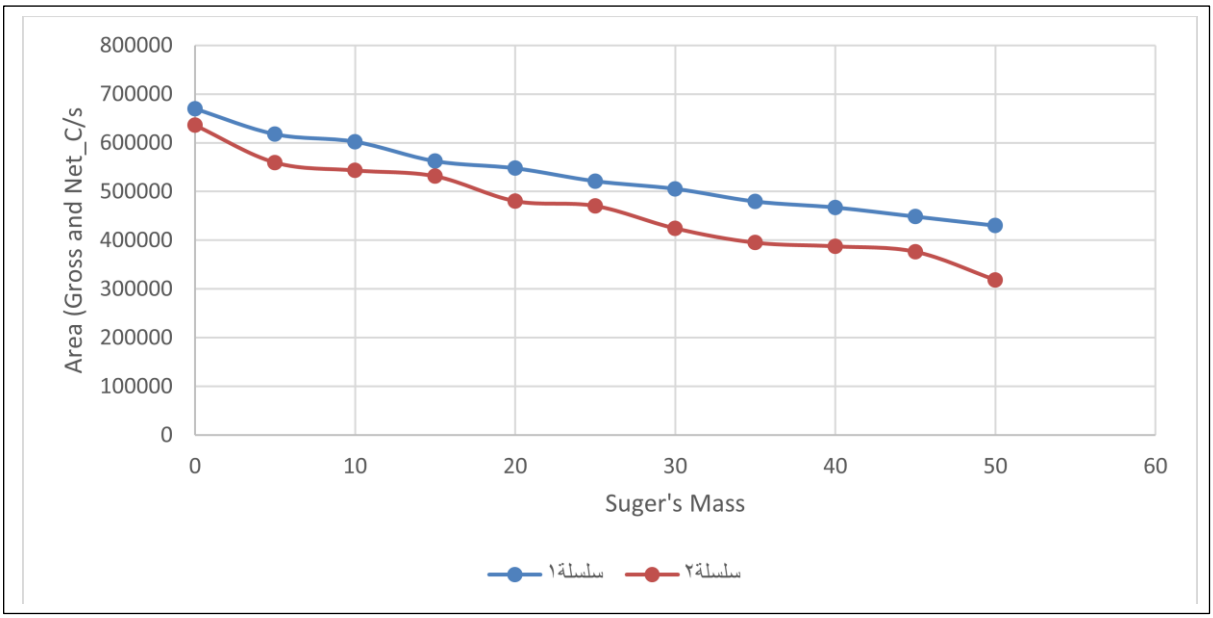

Figure (3-5): The relationship between the change in sugar concentration and the total area of the energy spectrum using a radioactive Cesium source.

Figure (3-5) shows the relationship between the mass of sugar added to $(300\,ml)$ of pure water on the total area of the radioactive cesium source spectrum for each of the total area of the spectrum (Gross Area) of the optical peak (the first series in blue) in addition to the net total area (Net Area) of the optical peak (in red). We note that the relationship was inverse, that is, with an increase in the sugar concentration, the total area (Gross and Net) of the spectrum decreases, because the absorbance of water for the radiation passing through it increases with the increase in the concentration of table salt in it, and this leads to a decrease in the total area of the energy spectrum.

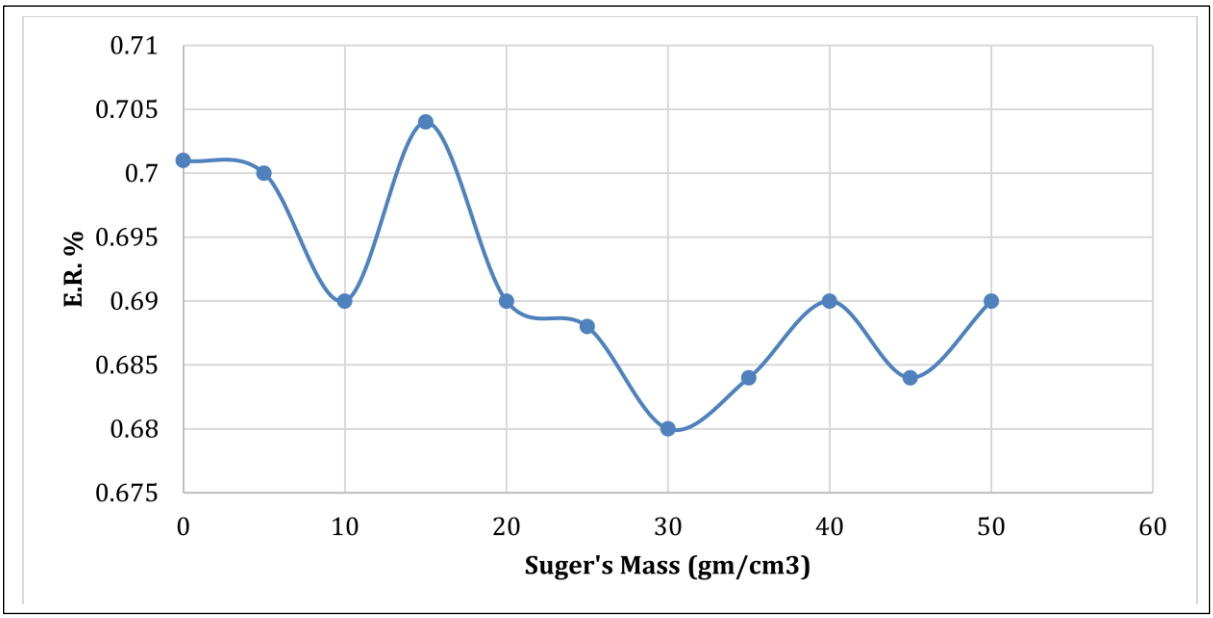

Figure (3-6): The relationship between sugar concentration change and the ability to analyze energy using a radioactive cesium source.

Figure (3-6) shows the relationship between the mass of sugar added to (300 ml) of pure water and the ability of analyze the energy of the radioactive cesium source spectrum, where we note that the relationship does not have a stable behavior and the reason may be due to environmental factors such as high temperature and humidity, which negatively affects the Crystallization of the NaI(Tl) detector, in addition to manual errors resulting from the inaccuracy in determining the area under the curve for each spectrum, which made it impossible to obtain a clear and more accurate relationship.

3.5 Study of the energy spectrum regions of gamma rays in sugar's mass using B- ^{60}Co source.

The gamma ray spectrum regions were studied using the ^{60}Co source at a distance of (2 cm) between the detector and the radioactive source, and (300 ml) of pure water was added to the sugar mass as in Table (3-4).

Table (3-4) The effect of the mass of sugar added to pure water on the absorption of gamma rays using a radioactive cobalt source

Mass (gm/cm^3)	Peak1(1173 keV)					Peak2(1332 keV)				
	Gross area (C/s)	Net area (C/s)	F.W.H.M	Ce.	E.R.%	Gross aera	Net area	F.W.H.M	Ce.	E.R.%
0	25146	16486	91.51	183	0.50	19936	14199	95.98	208	0.464
5	24835	14593	86.24	181	0.476	19224	13999	95.91	208	0.461
10	23870	14289	85.63	179	0.478	18865	12586	88.36	208	0.42
15	23208	13295	80.88	179	0.45	18560	22971	86.86	206	0.421
20	23121	13008	80.30	178	0.451	18382	11507	85.64	206	0.415
25	23109	12540	79.71	177	0.45	18267	11324	81.95	205	0.39
30	22765	12406	77.99	177	0.440	18160	10419	80.79	205	0.394
35	22450	11886	77.54	176	0.442	17903	10398	80.23	203	0.395
40	21845	10145	72.62	174	0.417	17878	9973	80.16	202	0.39
45	21305	9682	69.60	173	0.402	17724	8831	74.72	201	0.374
50	21294	9238	69.31	173	0.40	17539	8003	69.56	197	0.35

Table (3-4) shows the effect of the mass of sugar added to pure water on the absorption of gamma rays using the cobalt radioactive source, where the (Gross area) of the two peaks of energy ($1173\ keV$ and $1332\ keV$) as well as (Net area), in addition to (E.R.) were studied. We notice from the table how the mass of sugar added to ($300\ ml$) of pure water changes over the spectrum regions, as shown in Figures (3-7) and (3-8).

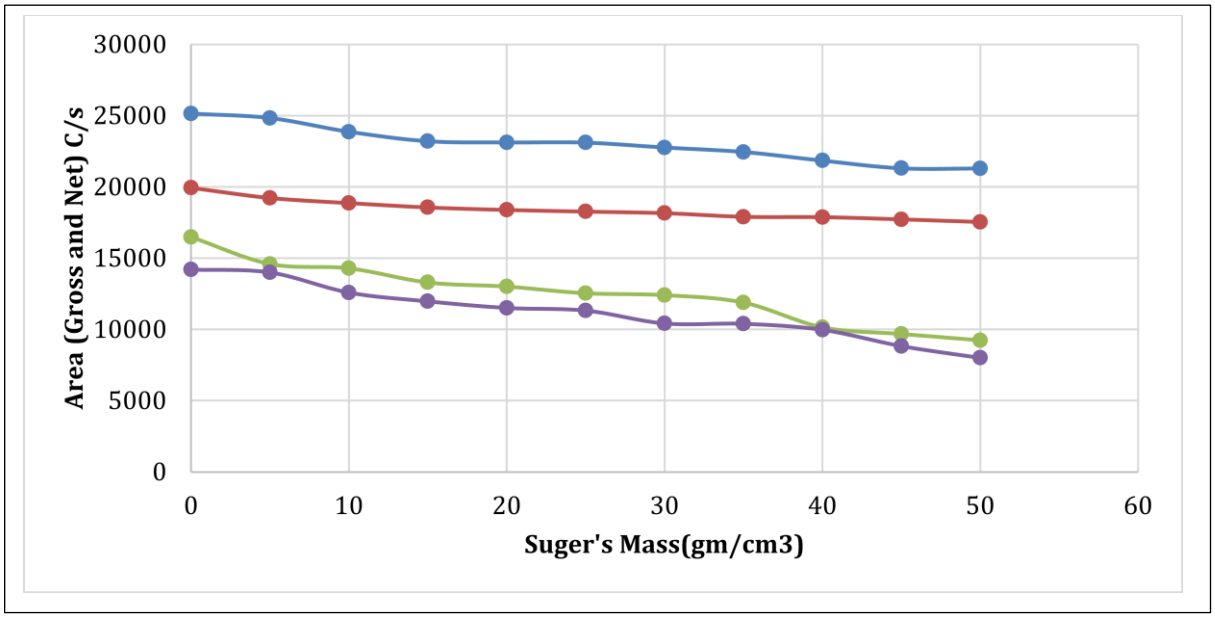

Figure (3-7): The relationship between the change in sugar concentration and the total area of the energy spectrum using a radioactive cobalt source.

Figure (3-7) shows the relationship between the mass of sugar added to (300 ml) of pure water on the net total area of the radioactive cobalt source spectrum for each of the total area of the spectrum (Gross Aera) for the first peak (in blue) as well as for the second peak in red In addition to the net optical area (Net Area) of the first two optical peaks (in green) and the second optical peak (in violet), where we note that the relationship was inverse between the concentration of table salt with the total area of the spectrum (Gross and Net), that is, by increasing the concentration, the total area of the spectrum decreases and for the same The reason is mentioned in Figure (1-3).

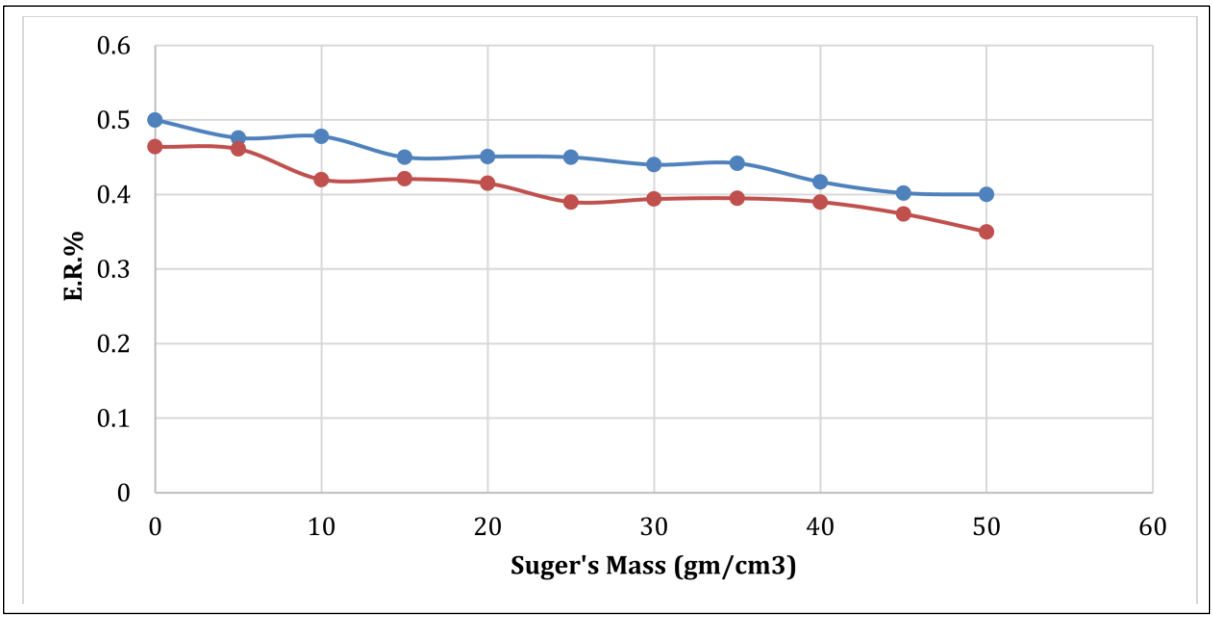

Figure (3-8): The relationship between sugar concentration change and the ability to analyze energy using a radioactive cobalt source.

Figure (3-8) shows the relationship between the mass of sugar added to ($300\ ml$) of pure water and the ability to analyze the energy of the cobalt source spectrum for the first (blue color) and the second (red color) peaks. As we note that the relationship is almost linear between the concentration of the additive and the ability to analyze energy, as increasing the concentration leads to a narrowing in the width of the middle of the top because the width of the middle of the top decreases with the increase in the concentration of salt added, but the location of the top was between constant and decrease with the increase in the concentration of added sugar.

Chapter Four

Conclusions and Future Work

4.1 Conclusions

1- With an increase in the concentration of table salt, the total area (Gross and Net) of the spectrum decreases, because the water's absorption of radiation passing through it increases with the increase in the concentration of table salt in it, and this leads to a decrease in the total area of the energy spectrum.

2- We note that the relationship is almost linear between the concentration of table salt added and the ability to analyze energy, as increasing the concentration leads to a narrowing in the width of the middle of the top because the width of the middle of the top decreases with the increase in the concentration of salt added.

3- There is an inverse relationship between the concentration of sugar and the total area (Gross and Net) of the spectrum, because the absorbance of water for the radiation passing through it increases with the increase in the concentration of sugar in it, and this leads to a decrease in the total area of the energy spectrum.

4- The relationship between the mass of sugar added to pure water and the ability to analyze the energy of the radioactive cesium source spectrum. Accuracy in determining the area under the curve for each spectrum, which made it impossible to obtain a clear and more accurate relationship.

4.2 Future work

1- Studying the effect of MnO_2 on the absorption of gamma ray using NaI(Tl) detector

2- Study the Air humidity in gamma-ray spectrum using NaI (Tl) detector.

References

[1] I. Rittersdorf, "Gamma ray spectroscopy," *Nucl. Eng. Radiol. Sci.*, pp. 18–20, 2007.

[2] M. F. L'annunziata, *Radioactivity: introduction and history, from the quantum to quarks*. Elsevier, 2016.

[3] T. Nakamura and T. Suzuki, "Monte Carlo calculation of peak efficiencies of Ge(Li) and pure Ge detectors to voluminal sources and comparison with environmental radioactivity measurement," *Nucl. Instruments Methods Phys. Res.*, vol. 205, no. 1, pp. 211–218, 1983.

[4] G. F. Knoll, "Radiation detection and measurement JOHN WILEY & SONS," *Inc., New York*, vol. 65, 2000.

[5] J. E. Martin, *Physics for radiation protection: a handbook*. John Wiley & Sons, 2006.

[6] J. Van der Steen *et al.*, "Strategies and Methods for Optimisation of Protection against Internal Exposures of Workers from Industrial Natural Sources (SMOPIE)," *NRG Rep.*, vol. 20790, no. 04.60901, 2004.

[7] O. B. Flores, A. M. Estrada, R. R. Suárez, J. T. Zerquera, and A. H. Pérez, "Natural radionuclide content in building materials and gamma dose rate in dwellings in Cuba," *J. Environ. Radioact.*, vol. 99, no. 12, pp. 1834–1837, 2008.

[8] T. Asano, K. Sato, and J. Onodera, "United nations scientific committee on the effects of atomic radiation 2000 report," *Japanese J. Heal. Phys.*, vol. 36, no. 2, pp. 149–158, 2001.

[9] M. I. Ojovan, W. E. Lee, and S. N. Kalmykov, *An introduction to nuclear*

waste immobilisation. Elsevier, 2019.

[10] T. F. Kraemer and D. P. Genereux, "Applications of uranium-and thorium-series radionuclides in catchment hydrology studies," in *Isotope tracers in catchment hydrology*, Elsevier, 1998, pp. 679–722.

[11] R. L. Grasty and J. R. LaMarre, "The annual effective dose from natural sources of ionising radiation in Canada," *Radiat. Prot. Dosimetry*, vol. 108, no. 3, pp. 215–226, 2004.

[12] M. Tufail, N. Akhtar, and M. Waqas, "Radioactive rock phosphate: the feed stock of phosphate fertilizers used in Pakistan," *Health Phys.*, vol. 90, no. 4, pp. 361–370, 2006.

[13] R. L. Mahler and A. Hamid, "Evaluation of water potential, fertilizer placement and incubation time on volatilization losses of urea in two northern Idaho soils," *Commun. Soil Sci. Plant Anal.*, vol. 25, no. 11–12, pp. 1991–2004, 1994.

[14] A. El-Taher, "Analytical methodology for the determination of concentration of pollutants and radioactive elements in phosphate fertilizer used in Saudi Arabia," 2013.

[15] I. Akkurt, K. Gunoglu, and S. S. Arda, "Detection Efficiency of NaI(Tl) Detector in 511–1332 keV Energy Range," *Sci. Technol. Nucl. Install.*, vol. 2014, p. 186798, 2014.

[16] S. Harb, N. K. Ahmed, and S. Elnobi, "Radon exhalation rate and radionuclides in soil, phosphate, and building materials," *J. Appl. Phys.*, vol. 7, no. 2, pp. 41–50, 2015.

[17] S. Saha, R. K. Singhal, H. Basu, and M. V Pimple, "Ammonium molybdate phosphate functionalized silicon dioxide impregnated in calcium alginate for

highly efficient removal of 137Cs from aquatic bodies," *RSC Adv.*, vol. 6, no. 98, pp. 95620–95627, 2016.

[18] B. M. Ladhaf and P. P. Pawar, "Effect of Absorber Concentration and Collimator Size on Gamma Ray Attenuation Measurements," *Int. J. Eng. Technol. Sci. Res.*, vol. 3, no. 3, 2016.

[19] T. Smith, S. Cao, and K. J. Kearfott, "Temporal Fluctuations in Indoor Background Gamma Radiation Using NaI(Tl)," *Health Phys.*, vol. 114, no. 3, 2018, [Online]. Available: https://journals.lww.com/health-physics/Fulltext/2018/03000/Temporal_Fluctuations_in_Indoor_Background_Gamma.13.aspx

[20] S. Suresh, D. R. Rangaswamy, E. Srinivasa, and J. Sannappa, "Measurement of radon concentration in drinking water and natural radioactivity in soil and their radiological hazards," *J. Radiat. Res. Appl. Sci.*, vol. 13, no. 1, pp. 12–26, 2020.

[21] A. S. Alaboodi, N. A. Kadhim, A. A. Abojassim, and A. B. Hassan, "Radiological hazards due to natural radioactivity and radon concentrations in water samples at Al-Hurrah city, Iraq," *Int. J. Radiat. Res.*, vol. 18, no. 1, pp. 1–11, 2020.

[22] G. Datar, G. Vichare, C. Selvaraj, A. Bhaskar, and A. Raghav, "Causes of the diurnal variation observed in gamma-ray spectrum using NaI (Tl) detector," *J. Atmos. Solar-Terrestrial Phys.*, vol. 207, p. 105369, 20209.

[23] L. M. Singh, K. Y. Singh, and A. K. Mahur, "Study of environmental radioactivity and radon measurement associated health effect due to coal and fly ash samples," *IOP Conf. Ser. Earth Environ. Sci.*, vol. 822, no. 1, p. 12026, 2021.

[24] M. S. Badawi, A. Hamzawy, and A. A. Thabet, “Hybrid analytical method for calibrating a standard NaI (Tl) gamma-ray scintillation detector using a lateral hexagonal radioactive source,” *AIP Adv.*, vol. 12, no. 6, p. 65021, 2022.

[25] A. A. Thabet and M. S. Badawi, “Analytical-numerical formula for estimating the characteristics of a cylindrical NaI(Tl) gamma-ray detector with a side-through hole,” *Nucl. Eng. Technol.*, 2022.

[26] T. Henriksen and D. H. Maillie, *Radiation and health*. CRC Press, 2002.

[27] N. Kruyts, Y. Thiry, and B. Delvaux, “Respective Horizon Contributions to Cesium-137 Soil-to-Plant Transfer: A Rhizospheric Experimental Approach,” Wiley Online Library, 2000.

[28] A. S. Rogowski and T. Tamura, “Environmental mobility of cesium-137,” *Radiat. Bot.*, vol. 10, no. 1, pp. 35–45, 1970.

[29] V. Winiarek, M. Bocquet, O. Saunier, and A. Mathieu, “Estimation of errors in the inverse modeling of accidental release of atmospheric pollutant: Application to the reconstruction of the cesium-137 and iodine-131 source terms from the Fukushima Daiichi power plant,” *J. Geophys. Res. Atmos.*, vol. 117, no. D5, 2012.

[30] A. D. Da Cruz, A. G. McArthur, C. C. Silva, M. P. Curado, and B. W. Glickman, “Human micronucleus counts are correlated with age, smoking, and cesium-137 dose in the Goiania (Brazil) radiological accident,” *Mutat. Res. Mutagen. Relat. Subj.*, vol. 313, no. 1, pp. 57–68, 1994.

[31] J. Van Dyk and J. J. Battista, “Cobalt-60: An old modality, a renewed challenge,” *Curr Oncol*, vol. 3, no. 10, 1996.

[32] J. L. Domingo, “Cobalt in the environment and its toxicological

implications," *Rev. Environ. Contam. Toxicol.*, pp. 105–132, 1989.

[33] J. F. Fowler Jr, "Cobalt," *Dermatitis*, vol. 27, no. 1, pp. 3–8, 2016.

[34] R. Lauwerys and D. Lison, "Health risks associated with cobalt exposure an overview," *Sci. Total Environ.*, vol. 150, no. 1–3, pp. 1–6, 1994.

[35] S. S. Kapoor and V. S. Ramamurthy, *Nuclear radiation detectors*, vol. 1. New Age International, 1986.

[36] G. Nelson and D. Reilly, "Gamma-ray interactions with matter," *Passiv. Nondestruct. Anal. Nucl. Mater.*, vol. 2, pp. 27–42, 1991.

[37] H. Seo *et al.*, "Multitracing capability of double-scattering Compton imager with NaI (Tl) scintillator absorber," *IEEE Trans. Nucl. Sci.*, vol. 57, no. 3, pp. 1420–1425, 2010.

[38] R. C. Hartman *et al.*, "Detection of high-energy gamma radiation from quasar 3C 279 by the EGRET telescope on the Compton Gamma Ray Observatory," *Astrophys. J.*, vol. 385, pp. L1–L4, 1992.

[39] D. V Gopinath and K. Gopala, "Analytical computation of the Compton continuum in gamma-ray spectrometry," *Radiat. Phys. Chem.*, vol. 56, no. 5–6, pp. 525–534, 1999.

[40] G. D. Palazzi, "High-energy bremsstrahlung and electron pair production in thin crystals," *Rev. Mod. Phys.*, vol. 40, no. 3, p. 611, 1968.

[41] E. Bellotti, C. Broggini, G. Di Carlo, M. Laubenstein, and R. Menegazzo, "Search for time dependence of the 137Cs decay constant," *Phys. Lett. B*, vol. 710, no. 1, pp. 114–117, 2012.

الخلاصة

لقد درسنا العلاقة بين تركيز ملح الطعام والسكر في الماء النقي وامتصاص أشعة جاما. تم الحصول على الإشعاع من مصادر مشعة وقياسه بواسطة كاشف NaI (Tl) وبرنامج Maestro من خلال دراسة أجزاء إعادة الانضمام في طيف الطاقة. وجدنا أن زيادة تركيز ملح الطعام مع المساحة الكلية (الإجمالي والصافي) للطيف يتناقص ، لأن امتصاص الماء للإشعاع الذي يمر عبره يزداد مع زيادة تركيز ملح الطعام فيه ، وهذا يؤدي إلى انخفاض في إجمالي مساحة طيف الطاقة. نلاحظ أن العلاقة خطية تقريبًا بين تركيز ملح الطعام المضاف والقدرة على تحليل الطاقة ، حيث تؤدي زيادة التركيز إلى تضييق عرض منتصف القمة لأن عرض منتصف القمة يتناقص مع زيادة تركيز الملح المضاف. توجد علاقة عكسية بين تركيز السكر والمساحة الكلية (الإجمالي والصافي) للطيف ، لأن امتصاص الماء للإشعاع الذي يمر به يزداد مع زيادة تركيز السكر فيه ، وهذا يؤدي إلى انخفاض في المساحة الإجمالية لطيف الطاقة. من ناحية أخرى ، تم العثور على العلاقة بين تركيز المادتين والقدرة على تحليل الطاقة لإظهار السلوك الخطي.

جمهورية العراق
وزارة التعليم العالي والبحث العلمي
جامعة بابل / كلية التربية للعلوم الصرفة – قسم الفيزياء

دراسة تاثير تراكيز السكر وملح الطعام في الماء على امتصاصية اشعة كاما باستخدام كاشف NaI (TI)

بحث مقدم الى كلية التربية للعلوم الصرفة بجامعة بابل
كجزء من متطلبات درجة الدبلوم العالي تربية/ فيزياء المواد وتطبيقاتها

من قبل

حوراء لطيف سلمان عباس

بكالوريوس تربية فيزياء
(جامعة القادسية ٢٠١٤ م)

اشراف

أ.م.د أنعام هاني كاظم

جامعة بابل - كلية التربية للعلوم الصرفة - قسم الفيزياء

١٤٤٤ هـ ٢٠٢٢ م